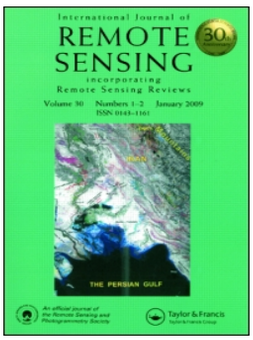

International Journal of Remote Sensing

ISSN: 0143-1161 (Print) 1366-5901 (Online) Journal homepage: https://www.tandfonline.com/loi/tres20

Assessment of different spectral indices in the red-near-infrared spectral domain for burned land discrimination

E. Chuvieco , M. P. Martín & A. Palacios

To cite this article: E. Chuvieco , M. P. Martín & A. Palacios (2002) Assessment of different spectral indices in the red-near-infrared spectral domain for burned land discrimination, International Journal of Remote Sensing, 23:23, 5103-5110, DOI: 10.1080/01431160210153129

To link to this article: https://doi.org/10.1080/01431160210153129

Published online: 25 Nov 2010.

INT. J. REMOTE SENSING, 2002, VOL. 23, NO. 23, 5103–5110

Assessment of different spectral indices in the red–near-infrared spectral domain for burned land discrimination

E. CHUVIECO†, M. P. MARTÍN‡ and A. PALACIOS†

†Departament of Geography, University of Alcalá, Colegios 2, 28801 Alcalá de Henares, Spain; e-mail: emilio.chuvieco@uah.es and alicia.palacios@uah.es
‡Institute of Economy and Geography (CSIC), Pinar 25, 28006 Madrid, Spain; e-mail: mpilar.martín@ieg.csic.es

(*Received 13 November 2001; in final form 25 April 2002*)

Abstract. A new spectral index named Burned Area Index (BAI), specifically designed for burned land discrimination in the red–near-infrared spectral domain, was tested on multitemporal sets of Landsat Thematic Mapper (TM) and NOAA Advanced Very High Resolution Radiometer (AVHRR) images. The utility of BAI for burned land discrimination was assessed against other widely used spectral vegetation indices: Normalized Difference Vegetation Index (NDVI), Soil Adjusted Vegetation Index (SAVI) and Global Environmental Monitoring Index (GEMI). BAI provided the highest discrimination ability among the indices tested. It also showed a high variability within scorched areas, which reduced the average normalized distances with respect to other indices. A source of potential confusion between burned land areas and low-reflectance targets, such as water bodies and cloud shadows, was identified. Since BAI was designed to emphasize the charcoal signal in post-fire images, this index was highly dependent on the temporal permanence of charcoal after fires.

1. Remote sensing of burned areas

The use of remote sensing for burned land assessment has grown notably in the last decade, and vast literature on this application is available. A simple classification of recent papers, highlights three lines of research (Chuvieco 1999, Ahern *et al.* 2001): (a) evaluation of new sensors, such as SPOT Vegetation, DMSP OLS and Terra Modis; (b) development or adaptation of methods for burned land discrimination, mainly interferometry, spectral unmixing, logistic regression and change detection analysis, and (c) spectral analysis of burned areas, to propose more accurate indices for burned land discrimination.

2. Objectives

This Letter aims to assess the accuracy of different vegetation indices for burned land mapping in both coarse and fine spatial resolution data. Although some authors have shown higher accuracies in the near-infrared and short wave infrared (NIR–SWIR) spectral domain for burned land discrimination (Pereira 1999, Trigg and Flasse 2001), only the indices based on the red and near-infrared region (R-NIR) have been assessed in this Letter. This decision was based on two grounds: first,

International Journal of Remote Sensing
ISSN 0143-1161 print/ISSN 1366-5901 online © 2002 Taylor & Francis Ltd
http://www.tandf.co.uk/journals
DOI: 10.1080/01431160210153129

there are still a wide range of sensors that are sensitive to those bands only (IRS WiFS, Resurs) and second, the availability of SWIR bands in satellite sensors is quite recent (1998 for SPOT HRV and Vegetation; 1999 for Modis, 2000 for NOAA AVHRR) and, therefore, for historical mapping of burned areas, the R-NIR range remains critical.

3. Methods

3.1. *Image pre-processing*

Six Landsat Thematic Mapper (TM) and two NOAA Advanced Very High Resolution Radiometer (AVHRR) images were used in this study. They correspond to pre-fire and post-fire conditions for several burned areas in Mediterranean countries. Landsat TM images of Italy (Island of Elba), Greece (near Athens) and Spain (Buñol, near Valencia), were acquired at different periods after a fire: 19 days (Buñol), 3 weeks (Athens) and 2 months (Elba). The time elapsed after the fire extinction is important for burned land discrimination, since the main spectral characteristics of burned areas change over short post-fire periods, from ash and charcoal during the first days/weeks to vegetation reduction in the following months (Pereira *et al.* 1999). In the case of NOAA AVHRR data, images were acquired a few days after large fires in the Iberian Peninsula during the 1994 summer.

All images were geometrically and radiometrically calibrated to compute reflectance using standard methods (Pons and Solé-Sugrañes 1994). On Landsat TM data, geometrical corrections were based on control points, whereas on AVHRR data orbital models were used with control points to increase multitemporal fitting precision.

3.2. *Indices tested*

Following previous burned land studies, three vegetation indices, based on the red–near-infrared spectral domain, were tested:

- The Normalized Difference Vegetation Index (NDVI), which has been extensively used in burned land discrimination (Fernández *et al.* 1997, Kasischke and French 1995).
- The Soil Adjusted Vegetation Index (SAVI: Huete 1988), which has shown to be very sensitive to discriminate vegetation amount in sparsely vegetated areas.
- The Global Environmental Monitoring Index (GEMI), claimed to be less affected by soil and atmospheric variations than NDVI (Pinty and Verstraete 1992). It has also proved to be more sensitive to burned area discrimination than NDVI (Pereira 1999).
- The Burned Area Index (BAI), defined by Martín (1998) specifically to discriminate fire-affected areas. This index is computed from the spectral distance from each pixel to a reference spectral point, where recently burned areas tend to converge:

$$\mathrm{BAI} = 1/((\rho c_{\mathrm{r}} - \rho_{\mathrm{r}})^2 + (\rho c_{\mathrm{nir}} - \rho_{\mathrm{nir}})^2) \quad (1)$$

where ρc_{r} and ρc_{nir} are the red and near-infrared reference reflectances, respectively, and ρ_{r} and ρ_{nir} are the pixel reflectances in the same bands. Values of ρc_{r} and ρc_{nir} were defined as 0.1 and 0.06, respectively, based on literature and analysis of several sets of satellite sensor images (Martín 1998). These values tend to emphasize the charcoal signal of burned areas.

3.3. *Index assessment*

To measure the discrimination ability of each spectral index, normalized distances (z) and transformed divergences (TD) were computed for images acquired after the fire and for the differences between pre- and post-fire images. These measurements were calculated using a sample of 500–1000 random points (depending on the image size) extracted from the images. Average values for NDVI, SAVI, GEMI and BAI (and the temporal differences) were computed for each land cover type, as well as for burned areas. The discrimination ability of each index was measured by the average z distances from burned areas to all other land cover types, as well as the TD values between pairs of classes (burned areas and any other land cover type).

In addition, a simple thresholding technique was applied to each spectral index to assess its spatial discrimination potential. Thresholds were defined as the average-minus-one standard deviation for NDVI, SAVI and GEMI, and plus one standard deviation for BAI. These thresholds were applied to both post-fire Landsat TM images and to temporal differences. Thresholds were defined to reduce commission errors (unaffected pixels flagged as burned), which are usually the most critical in burned land mapping applications. Commission errors were evaluated by comparing burned-classified pixels with fire perimeters derived from visual interpretation of Landsat TM images.

4. Results

Grey displays of NDVI, SAVI and GEMI showed similar patterns for burned areas, although a higher contrast with unburned areas is observed in GEMI (figure 1). Unlike the other indices, BAI shows the highest values for burned areas, clearly separating before/after situations.

BAI presents the most distinct values for burned areas in the post-fire image, as well as in temporal differences (figure 2). However, this index also shows an important variability, with a variation coefficient near 40% (figure 3). This refers to the spatial variability of burned areas, which may be closer or further away from the convergence point depending on fire severity, or the density of pre-fire vegetation. In contrast, GEMI offers the lowest variation coefficient, which implies a lower discrimination sensitivity to internal variations within the burned areas, but a greater ability to separate burned areas from other covers. Similar trends were observed in NOAA AVHRR data.

The high variability of BAI values explains low z distances compared with other indices (table 1). However, the highest and second highest z values were obtained with BAI for Elba and Athens, respectively. Both images were acquired at later dates from the fire occurrence than in the Buñol site and, therefore, BAI variability was lower, since short-term differences in burned areas were removed. Temporal differences showed similar trends, although BAI offers the highest z distances in the Athens image also. In spite of Buñol having lower z values, TD values between burned areas and other land covers are higher for BAI than for the other indices, providing the highest divergence from burned areas in four out of eight land covers in post-fire images and six out of eight for temporal differences (table 2).

For AVHRR data, normalized distance was calculated using a single post-fire image acquired several weeks after the fires. In table 3, BAI shows the largest distance between burnt areas and other land covers except water bodies. The coarse spatial resolution of AVHRR imagery limits the detection of local-scale variability within

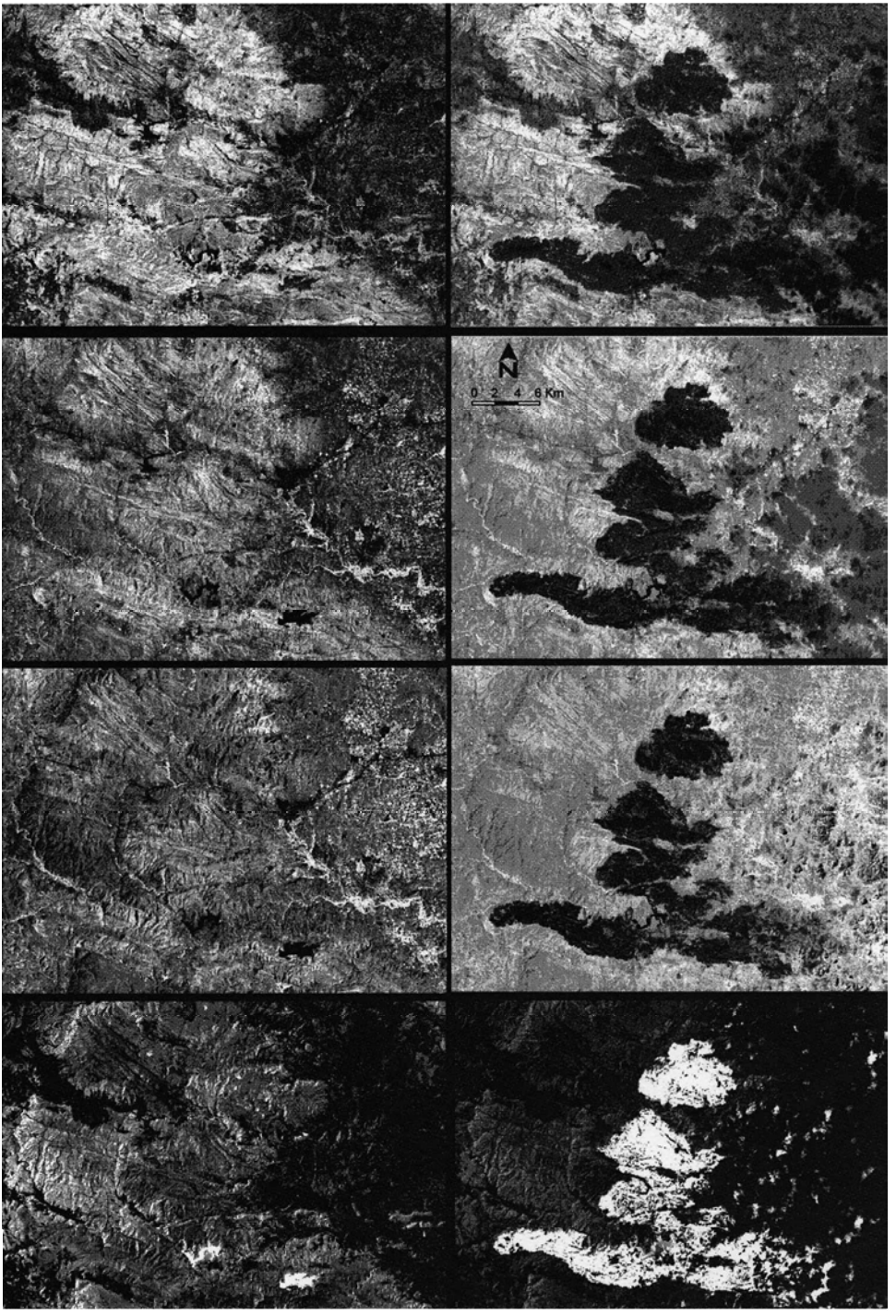

Figure 1. Spectral indices derived from Landsat TM images from before (left) and after (right) a large fire in Buñol (Valencia, Spain). From top to bottom: NDVI, SAVI, GEMI and BAI.

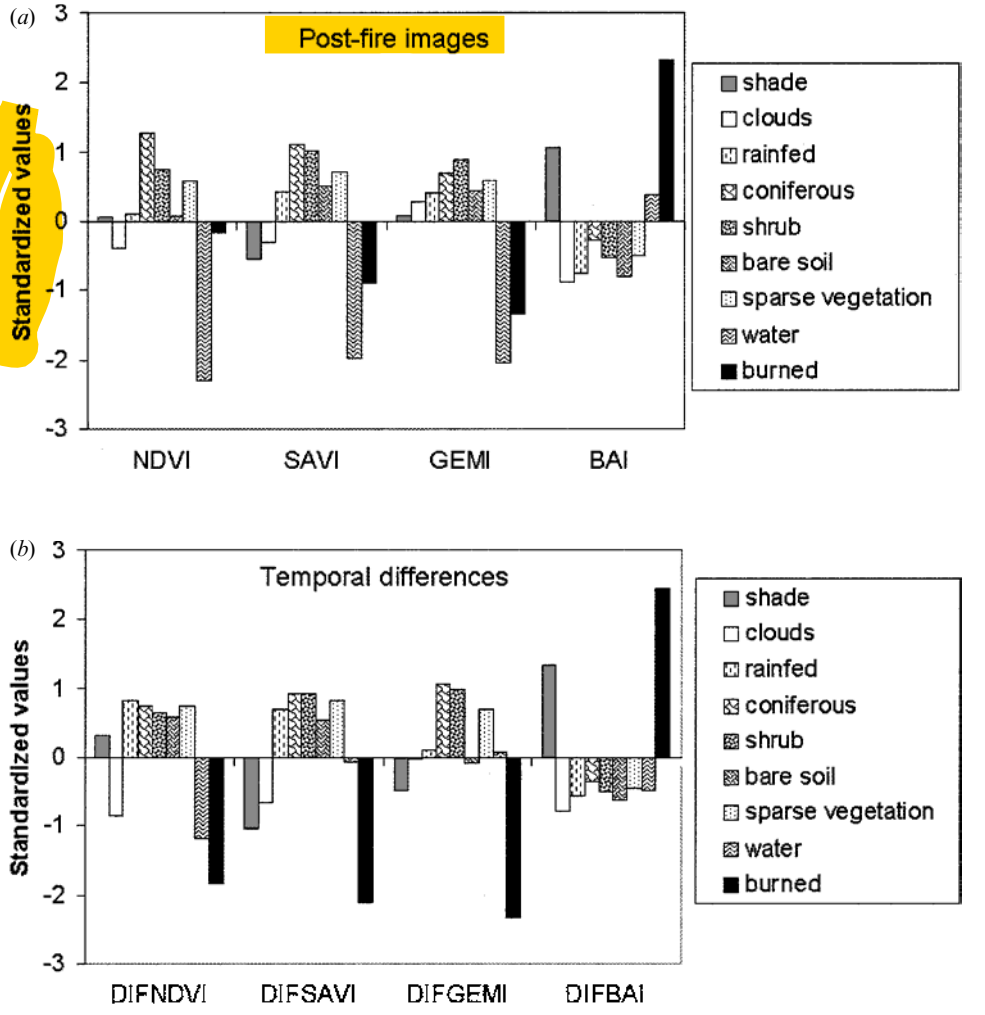

Figure 2. Average standardized values ((value–mean)/standard deviation) of the different spectral indices for the land covers of Buñol site (Landsat TM data). DIFNDVI, DIFSAVI, DIFGEMI and DIFBAI refer to the temporal difference of NDVI, SAVI, GEMI and BAI values, respectively.

the fires. Therefore, burned land variance in BAI values is also lower than for Landsat TM data and the z distances are higher.

Figure 4 shows the pixels detected as burned areas using thresholds of Landsat TM post-fire and temporal difference images. BAI has few commission errors, although some problems were found in coastal areas, where land/water interactions occur. This is also the case for NDVI, SAVI and GEMI. NDVI and GEMI show some confusion with clouds and shadows in Buñol and Athens, while SAVI only has some errors in sparsely vegetated areas.

5. Conclusions

BAI shows a high discrimination ability for burned areas in the R-NIR spectral domain, being more sensitive to burnt areas than NDVI, GEMI and SAVI. However,

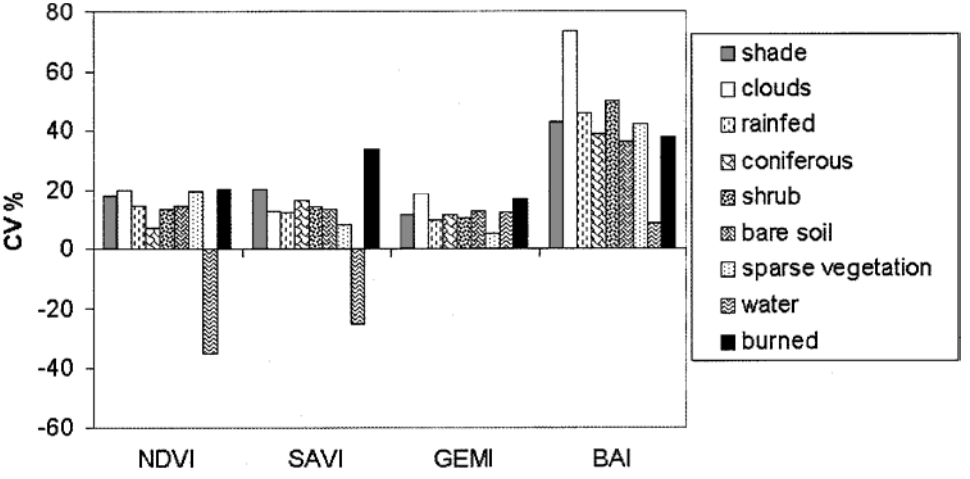

Figure 3. Coefficients of variation for the different spectral indices for the Landsat TM post-fire images in Buñol.

Table 1. Average z distances between burned areas and other land covers (Landsat TM).

	Post-fire values				Temporal differences			
	NDVI	SAVI	GEMI	BAI	NDVI	SAVI	GEMI	BAI
Athens	1.89	2.30	1.80	2.00	1.80	1.64	1.76	1.98
Buñol	1.93	2.45	2.89	1.97	2.18	2.49	2.63	1.96
Elba	1.14	1.32	1.33	1.34	1.13	1.02	0.94	1.13

Table 2. Index with highest transformed divergence values from burned areas to other land covers (Landsat TM data, Buñol site).

	Post-fire image	Temporal differences	Both
Shade	GEMI	DIFNDVI	GEMI
Clouds	BAI	DIFBAI	DIFBAI
Rain-fed crops	BAI	DIFBAI	DIFBAI
Coniferous	NDVI	DIFBAI	DIFBAI
Shrubs	BAI	DIFBAI	DIFBAI
Bare rock	BAI	DIFBAI	DIFBAI
Sparse vegetation	NDVI	DIFBAI	DIFBAI
Water bodies	NDVI	DIFNDVI	NDVI

Table 3. Normalized distance between burned areas and other land covers in NOAA AVHRR post-fire image.

	NDVI	GEMI	SAVI	BAI
Water	1.86	4.80	1.90	4.66
Cloud shadows	1.37	0.67	1.33	2.19
Forest	3.46	3.10	3.48	5.55
Shrubs	2.92	4.52	2.97	5.90
Non-irrigated crops	1.70	3.92	1.74	9.23

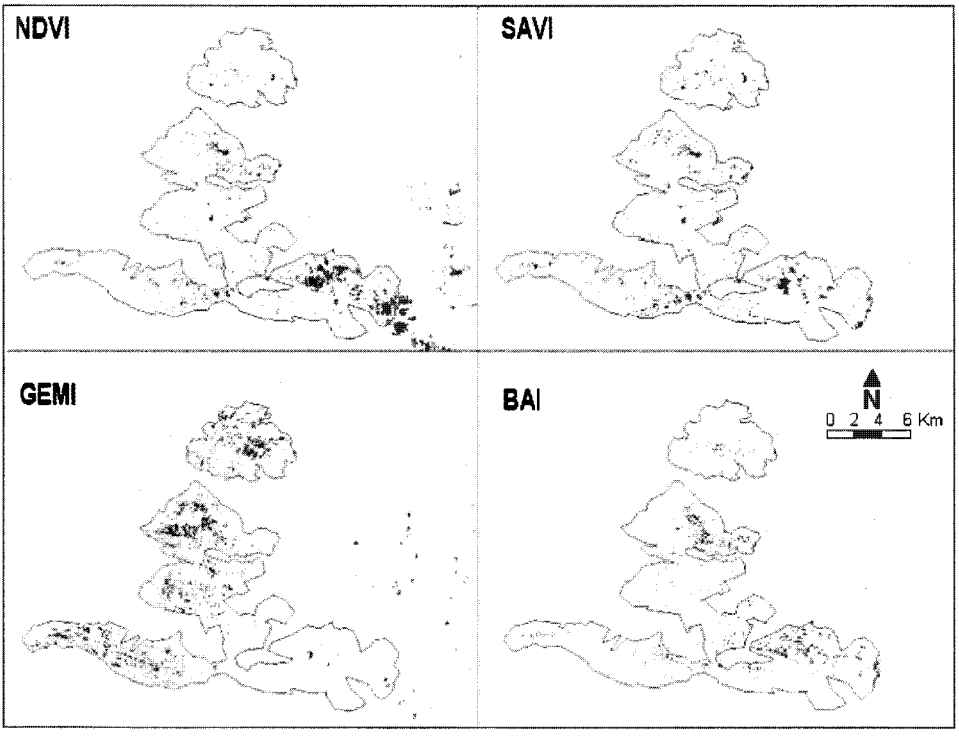

Figure 4. Burned land pixels extracted from thresholds of post-fire and temporal change images in the Buñol study site. Fire perimeter is included for reference.

since this index was designed to emphasize charcoal in post-fire images, it presents some potential confusion with low-reflectance targets, such as water bodies or cloud shadows. For burned land mapping, thresholds for this index should be very severe since BAI shows a high variability within scorched areas. The index discriminates consistently burned areas where charcoal signal prevails. Therefore, it may be very useful to group burned land mapping in two phases: in the first one, only 'core' pixels within burn scars would be discriminated, while in the second a shape refinement algorithm could be applied to refine identification of burned surfaces.

Finally, it should be emphasized that BAI has been developed for Mediterranean environments. Its applicability to other biomes largely depends on charcoal endurance after the fire, which may ranges from months (boreal regions) to weeks or days (tropics).

References

AHERN, F. J., GOLDAMMER, J. G., and JUSTICE, C. O. (eds), 2001, *Global and Regional Vegetation Fire Monitoring from Space: Planning a Coordinated International Effort* (The Hague, The Netherlands: SPB Academic Publishing).

CHUVIECO, E. (ed.), 1999, *Remote Sensing of Large Wildfires in the European Mediterranean Basin* (Berlin: Springer).

FERNÁNDEZ, A., ILLERA, P., and CASANOVA, J. L., 1997, Automatic mapping of surfaces affected by forest fires in Spain using AVHRR NDVI composite image data. *Remote Sensing of Environment*, **60**, 153–162.

HUETE, A. R., 1988, A soil-adjusted vegetation index (SAVI). *Remote Sensing of Environment*, **25**, 295–309.

KASISCHKE, E., and FRENCH, N. H., 1995, Locating and estimating the areal extent of wildfires in Alaskan boreal forest using multiple-season AVHRR NDVI composite data. *Remote Sensing of Environment*, **51**, 263–275.

MARTÍN, M. P., 1998, Cartografía e inventario de incendios forestales en la Península Ibérica a partir de imágenes NOAA AVHRR. Doctoral thesis, Universidad de Alcalá, Alcalá de Henares.

PEREIRA, J. M. C., 1999, A comparative evaluation of NOAA AVHRR vegetation indices for burned surface detection and mapping. *IEEE Transactions on Geoscience and Remote Sensing*, **37**, 217–226.

PEREIRA, J. M., SA, A. C. L., SOUSA, A. M. O., SILVA, J. M. N., SANTOS, T. N., and CARREIRAS, J. M. B., 1999, Spectral characterisation and discrimination of burnt areas. In *Remote Sensing of Large Wildfires in the European Mediterranean Basin*, edited by E. Chuvieco (Berlin: Springer), pp. 123–138.

PINTY, B., and VERSTRAETE, M. M., 1992, GEMI: a non-linear index to monitor global vegetation from satellites. *Vegetatio*, **101**, 15–20.

PONS, X., and SOLÉ-SUGRAÑES, L., 1994, A simple radiometric correction model to improve automatic mapping of vegetation from multispectral satellite data. *Remote Sensing of Environment*, **48**, 191–204.

TRIGG, S., and FLASSE, S., 2001, An evaluation of different bi-spectral spaces for discriminating burned shrub-savannah. *International Journal of Remote Sensing*, **22**, 2641–2647.